CONSTRAINING THE SIZE OF THE SOUTH POLE-AITKEN BASIN IMPACT. R. W. K. Potter[1], G. S. Collins[1], D.A. Kring[2] , W. Kiefer[2] , P. McGovern[2], [1]Impacts and Astromaterials Research Centre, Dept. Earth Science and Engineering, Imperial College London, London, SW7 2AZ, UK, ross.potter04@imperial.ac.uk; [2]Lunar and Planetary Institute, 3600 Bay Area Blvd, Houston, TX, 77058, USA

Introduction: The 2500km diameter [1] South Pole-Aitken (SPA) basin is the largest and oldest impact structure on the Moon. The scale of the impact suggests that normally inaccessible lunar material, such as deep crust or mantle, was excavated or uplifted to the lunar surface, making SPA a strong candidate for possible sample return missions [2]. Analysis of originally deep-seated material would help further our understanding of planetary differentiation and early Solar System processes.

Crater scaling arguments [3] and previous numerical modeling of giant impacts on the Moon [4, 5, 6] suggest that an SPA-scale impact would bring impact-processed mantle material to the lunar surface; either by ejection or by uplift as part of the rebounding crater floor. SPA-scale impact models also predict the production of a large melt pool underneath the central crater basin. Many spectroscopic studies of the basin have been undertaken [7, 8], with [8] suggesting that the basin floor has a composition best described as a mixture of lower crustal and mantle material. Gravity data, tied to constraints on crustal structure from Apollo seismic data suggest that the SPA basin is underlain by a ~10-30km-thick layer, less dense than the mantle, which thins toward the crater center [9].

A working hypothesis that synthesizes all these observations is that the SPA-impact excavated the majority (if not all) of the lunar crust from the basin floor and generated a large central pool of molten mantle (and, perhaps, some lower crust). This melt-pool then differentiated, cooled and recrystallised to leave a low-density surface layer with a composition intermediate to that of pure lower crust and pure mantle [10]. If this hypothesis is correct, the dimensions of the compositional anomaly in the SPA basin and gravity data provide constraints on the dimensions and shape of the melt pool and surrounding variations in crustal thickness. Here, we use these constraints to refine hydrocode simulations of the SPA impact based on model predictions of the volume, dimensions and final location of the melt pool and crustal deformation.

Methods: We used the two-dimensional iSALE hydrocode [11,12] to simulate vertical impacts at 10-20 km/s of asteroids 100-200-km diameter into a spherical Moon with a resolution of 3km per cell (30-60 CPPR; e.g., Fig. 1). The Moon was modelled as a three-layer globe, 1749km in radius, consisting of a 48-km thick crust, mantle and core. ANEOS-derived equation of state tables for dunite [13] and iron [14] were used to represent the mantle and core, respectively. The Tillotson equation of state, with parameters determined for gabbroic anorthosite [15], was used to model the crust. Dunite was also used to represent the impacting asteroid. Strength and thermal model parameters for both dunite and gabbroic anorthosite were calculated from experimental data [16, 17, 18, 19].

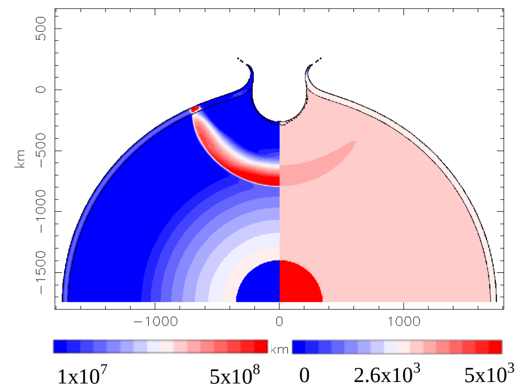

Figure 1: The shock wave 1.6 mins after impact at 10 km/s of a 150-km diameter projectile into the Moon. The left panel shows strength; the right panel shows density. Prior to impact, the upper mantle temperature is close to the melt temperature, giving it almost zero strength.

Self-consistent initial gravity, pressure, strength and density fields within the Moon were computed based on a prescribed radial thermal profile, representing lunar conditions at the time of impact. As a first approximation, the temperature in the Moon was assumed to increase with depth by 25K/km in the crust and upper mantle, and follow an adiabatic temperature gradient in the mantle and core, pinned at a temperature of 1740K at a depth of 560km. The temperature profile was also bounded by the solidus (from the crust-mantle boundary to a depth of 560km) so that the mantle temperature was not above the melting point at any location. The gravity field above the surface of the Moon decayed in magnitude with radial distance squared. The gravity field over the whole mesh was fixed during the simulation; no account was taken for the change in the gravity field caused by the redistribution of mass by the impact.

Results: Figure 2a shows the final crater structure and melt fraction from an example simulation (150km diameter; 10km/s). Two distinct zones were created following the impact (Fig. 2b); the first zone is ~800km wide and contains a deep melt pool of partially molten mantle material. This zone is approximately equal in size to the transient crater (diameter ~900km) and contains little, if any, crustal material. At a diameter of ~800km, a second zone begins; here crustal material underlies partially molten mantle material to a diameter of ~2000km. In this case, partially molten mantle material was exhumed to the lunar surface by both ejection and run-off from the central uplift. Molten mantle material will have been ejected to localities farther from the impact site; however, our simulations did not resolve this material. Mantle material was melted through one of two processes; shock heating or decompression melting. According to the prescribed thermal profile, upper mantle material is at or very near to the solidus before impact. Consequently, only a small decrease in pressure will cause partial melting. The total volume of mantle melt created by the impact was calculated to be 5.9×10^7 km^3. This compares to a value of 2.6×10^7 km^3 for a chondrite impactor impacting at 10 km/s using standard scaling laws for melt production [20]. The volume difference is due to two factors: 1) upper mantle material being at or near to the solidus pre-impact, and 2) uplifted mantle melted by decompression. At higher impact velocity more material will be melted through the shock heating mechanism.

Discussion: The old age, large size and severe degradation of the SPA basin, combined with a lack of direct sampling, mean an accurate reconstruction of the impact is extremely difficult. However, our model results can be compared directly to observational data to help establish the scale of the SPA impact and test the model.

The compositional anomaly at SPA is approximately equal to its observed diameter (2500km). If the compositional anomaly is related to the presence of partially molten upper mantle on the lunar surface, the example simulation presented here predicts a compositionally anomalous zone ~2000km in diameter. Moreover, analysis of Clementine data suggests that later impacts in the outer part of the SPA basin have exposed buried upper crustal anorthosite; whereas, there is no evidence of upper crustal anorthosite exposures within an inner diameter of 1260 km [21]. The model results in Fig. 2 show no upper crustal material inside a diameter of ~800km. Together, these comparisons suggest that the SPA impact was more energetic than our example; however, further simulations, examining different thermal profiles and impact parameters are required to confirm this.

Acknowledgements: RWKP and GSC are grateful for NSLI travel support allowing them to carry out research at the LPI-JSC Center for Lunar Science and Exploration, NASA Lunar Science Institute. We thank Boris Ivanov, Jay Melosh, Kai Wünnemann and Dirk Elbeshausen for their work in the development of iSALE. RWKP and GSC were both funded by NERC.

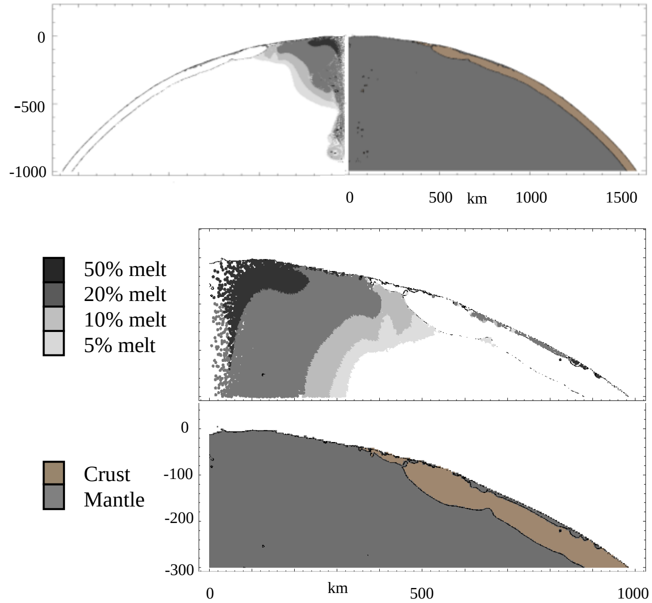

Figure 2: **(a)** The extent of molten mantle material (left panel) and, mantle and crustal material (right panel) at the end of the simulation, **b)** the two zones created in the impact: an ~800km diameter mantle melt pool, with no crust present, and a second zone where crustal material underlies partially molten mantle to a diameter of ~2000km.

References: [1] Wilhelms, D. E. (1987) *The Geologic History of the Moon*, U.S Government Printing Office, Washington, D. C. [2] National Research Council (2007) *The scientific context for the exploration of the moon*, National Academies Press, Washington D.C. [3] Croft, S.K. (1978), *Proc. LPSC. IX*, 3711-3733. [4] Collins, G.S & Melosh, H.J. (2004) *LPSC XXXV*, abstract #1375. [5] Ivanov, B.A. (2007) *LPSC. XXXVIII*, abstract #2003. [6] Hammond, N.P. et al (2009) *LPSC XL*, abstract # 1455. [7] Pieters et al (1997) *GRL*, 24, 1903-1906 [8] Lucey, P.G. et al (1998) *JGR.* 103, 3701-3708. [9] Hikida, H. & Wieczorek, M.A. (2007) *Icarus*, 192, 150-166 [10] Morrison, D.A. (1998) *LPSC*. XXIX, abstract #1657. [11] Collins, G.S. et al (2004) *MAPS* 39, 217-231 [12] Amsden, A. A., et al (1980) *Los Alamos National Laboratory Report LA-8095* [13] Benz, W. et al (1989) *Icarus*, 81, 113-131 [14] Thompson, S.L. & Lauson, H.S. (1972) *Sandia National Laboratory Report SC-RR-71 0714* [15] O'Keefe, J.D. & Ahrens, T.J. (1982) *Geol. Soc. Am. Spec. Pap.*, 190, [16] Azmon, E. (1967) *NSL 67-224.* [17] Stesky R. M. et al (1974) *Tectonophys.* , 23, 177–203. [18] Shimada, M. et al (1983) *Tectonophys*, 96, 159-172. [19] Ismail, I.A.H. & Murrell, S.A.F (1990) *Tectonophys*, 175, 237- 248. [20] Cintala, M.J., & Grieve, R.A.F.(1998) *MAPS*, 33, 889-912 [21] Petro, N.E. & Pieters, C.M. (2002) *LPSC* XXXIII, abstract #1848.